

## Gigacycle Fatigue of Metallic Aircraft Components

Claude Bathias<sup>1</sup> and Paul C. Paris<sup>2</sup>

<sup>1</sup> Professor, LEEE/ITMA University Paris X at Ville d'Avray (Fr)

<sup>2</sup> Visiting professor, LAMEFIP, ENSAM, Bordeaux (Fr)

claude@bathias.com, pcp@me.wustl.edu

**Keywords:** Gigacycle fatigue, prediction, modeling, aeronautical materials, damage tolerance.

**Abstract.** According to the Paris-Hertzberg crack growth law, an analytical model shows that cracks grow from a flaw very quickly from short crack to long cracks, in the gigacycle fatigue. The location of the initiation, at the surface or inside, has a small effect. This means that the key problem is the nucleation of the crack from the flaws as it is shown by P. Lukas and H Mughrabi. (1-2) This approach is applied to a PM Ni alloy.

### Introduction

When A. Wohler suggested the first basic approach of the S-N fatigue life of metals, the main industrial applications were rail car axels and steam engines for railways and boats. The slow rotation of a steam engine was about 50 cycles per minute, more or less. Thus, the fatigue limit was defined by Wohler between  $10^6$  and  $10^7$  cycles. Now, the fatigue life of an automobile engine is ranging in the gigacycle  $10^9$ , regime and the aircraft turbine is of the order of  $10^{10}$  cycles, according to rotation of several thousands per minute. (3-4)

It is relevant to notice that an airplane is a complex machine where low cycle fatigue is damaging turbine disks but blade vibrations produce Gigacycle fatigue. The fuselage and the wings are mainly loaded in megacycle fatigue.

Among the three fatigue regimes, very high fatigue life is certainly the newest area of study. In this paper we give the results of gigacycle fatigue of several aeronautical alloys: aluminium, titanium, nickel based alloys and high strength steels used in aircraft industry Safe-life design based on the infinite-life criterion was initially developed in the 19th century, the prime example is the stress-life or S-N approach is related to the asymptotic behaviour of low strength steels. Some materials display an apparent fatigue limit stress level at a high number of cycles. Other materials do not exhibit such a limit, but instead display a continuously decreasing stress-life S-N curve, even at a great number of cycles than  $10^9$  cycles. This is the case for aluminium, titanium, nickel alloys and high strength steels.

All cracks nucleate in the gigacycle regime at microscopic flaws and defects. Depending on the processing different types of flaws are critical: pores in castings, pores and inclusions in powder metallurgy, inclusions in forging and sometimes grain size.

As mentioned before, many components in aircrafts are submitted to vibration that is to say: the gigacycle regime. In this paper, the study of a nickel based alloy (N18) has been chosen in order to illustrate such problem for aircraft turbine disc. Usually this type of component is design only in low cycle fatigue since vibration is neglected. However, initiation in VHCF due to flaws is a real danger. In order to determine the form of the S-N curve between  $10^6$  and  $10^9$  cycles, it is necessary to apply an accelerated fatigue testing method based on ultrasonic technique operating at 20kHz.

**Crack growth from a flaw**

Paris and al.-2004 have shown a historical review on crack growth and threshold to develop the estimation procedure for crack growth life for internal initiation, termed “fish-eye”. Here, as in that work, the observations and analysis made in the early 1960s, resulted in Paris-1999, and Hertzberg-1993, 1995, 1997 which predict the threshold corner at:

$$\frac{da}{dN} = b \quad \text{and} \quad \frac{\Delta K_{eff}}{E\sqrt{b}} = 1$$

Where *b* is the Burger’s vector and *E* is elastic modulus.  $\Delta K_{eff}$  is the non-closer value of  $\Delta K$ , the crack tip stress intensity factor. The corresponding crack growth law is used to estimate the life of the small cracks in the fish-eye range, considering that crack closure is minimal for this type of crack:

$$\frac{da}{dN} = b \left( \frac{\Delta K_{eff}}{E\sqrt{b}} \right)^3$$

Later in the 1990s, Paris-1999 and Hertzberg-1996, 1997, and others have shown the effectiveness of this relationship, and above history as a predictor of the threshold corner and slope, see figure 1.

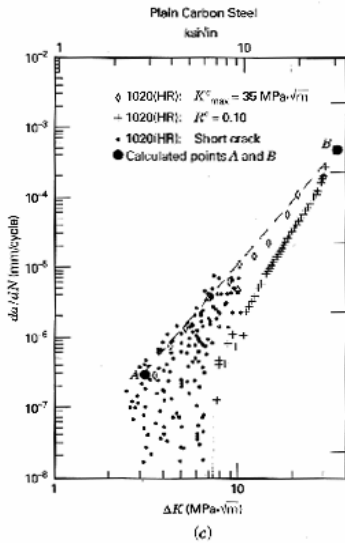


**Figure 1:** Hertzberg results. Short crack effect on fatigue propagation

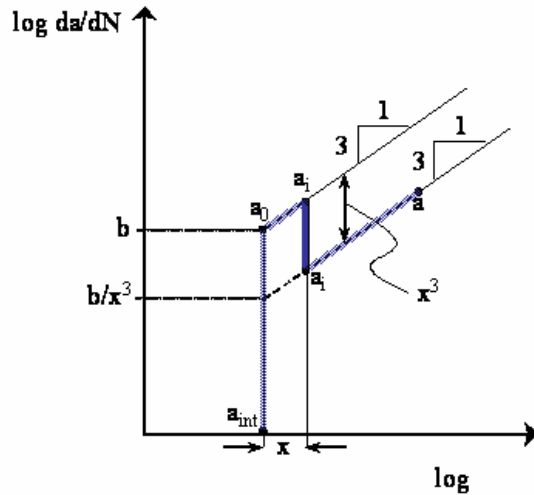


**Figure 2:** Modeling of the short crack effect for an internal circular crack

The initiation from an inclusion or other defect itself must be close to the total life, perhaps much more than 99% of the life in most cases. This can be made evident by integrating the fatigue crack growth rates for small cracks to estimate the possible extent of crack growth life.

In order to do this one should refer to the general behavior pattern of the crack growth rate curve as illustrated by the equations preceding. It is noted that small cracks such as those growing from small inclusions do not exhibit crack closure so these equations in terms of  $\Delta K_{eff}$  apply very well. They form an upper bound on crack growth rates for the small cracks in the “fish eye” size range for which crack closure is minimal, see figures 2 and 3.

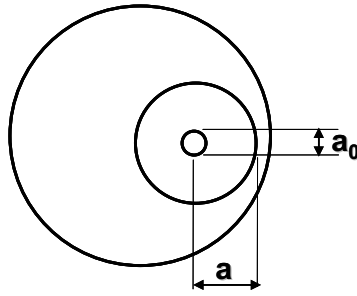


Figure 3 Fish eye model for gigacycle initiation

Estimating the life for a crack of this type beginning just above threshold it is then appropriate to consider the growth law as:

$$\frac{da}{dN} = b \left( \frac{\Delta K_{eff}}{E\sqrt{b}} \right)^3$$

Where for the circular crack growing in a “fish eye” the stress intensity factor formula is:

$$\Delta K = \frac{2}{\pi} \Delta\sigma \sqrt{\pi a}$$

The integration of the Paris Hertzberg law without transition, to determine the crack growth life will begin here with the crack growth rate threshold corner which we shall denote as  $\Delta K_0$  corresponding to an initial circular crack of radius,  $a_0$ . Substituting these into the first formula here we obtain:

$$\frac{da}{dN} = b \left( \frac{\Delta K_0}{E\sqrt{b}} \right)^3 \left( \frac{a}{a_0} \right)^{3/2} = b \left( \frac{a}{a_0} \right)^{3/2}$$

This equation can be integrated from  $a_0$  to  $a_{final}$  which gives:

$$N_f = \int_{a_0}^{a_f} \frac{(a_0)^{3/2}}{b} \cdot \frac{da}{(a)^{3/2}} = \frac{2(a_0)^{3/2}}{b} \left[ \frac{1}{(a_0)^{1/2}} - small \right] \cong \frac{2a_0}{b}$$

But it can be noted that:

$$1 = \frac{\Delta K_0}{E\sqrt{b}} = \frac{2\Delta\sigma\sqrt{a_0}}{\sqrt{\pi E}\sqrt{b}} \quad a_0 = \frac{\pi E^2 b}{4(\Delta\sigma)^2}$$

Thus leading to the following formula:

$$N_f = \frac{\pi E^2}{2(\Delta\sigma)^2}$$

This is the result for the approximate number of cycle from the threshold corner to failure from an initial crack size  $a_0$  as expressed above(3).

$E$  = Dynamic Young's modulus at 20 kHz

$\Delta\sigma$  = experimental nominal stress

$N_f = N_{fish-eye} = N_{total}$

Estimating the crack growth life for a internal "fish-eye" crack beginning just above threshold it is then appropriate to consider the growth life ( $N_{fish-eye}$ ) for a internal "fish-eye". This shall be defined considering its respective portion of life, from threshold corner ( $N_{total}$ ) when it is small crack ( $N_{a_0 \rightarrow a_i}$ ) and when it changes to large crack ( $N_{a_i \rightarrow a}$ ), and its respective crack growth life below threshold ( $N_{int}$ ):

$$N_{fish-eye} = N_{total} + N_{int}$$

$$N_{total} = N_{a_0 \rightarrow a_i} + N_{a_i \rightarrow a}$$

The integration to determine the small crack growth life will begin here with the crack growth rate corner which we shall denote as  $\Delta K_\theta$  corresponding to an initial circular crack of radius,  $a_0$ , until a circular crack of radius,  $a_i$ , (transition of small crack to large crack).

The integration to determine the below threshold crack growth life can be estimated by the law used above, from an initial flaw,  $a_{int}$  to  $a_0$  at the threshold corner; but prior to the corner threshold should have a very much higher slope  $\alpha$ .

The result to estimate the total crack growth lifetime for an internal failure "fish-eye", which is the addition of follow lifetime:

- Below threshold, from an initial flaw,  $a_{int}$  to  $a_0$
- Small crack, from an initial circular crack of size,  $a_0$  to  $a_i$
- Large crack, from transition small to large crack point,  $a_i$  to  $a$

$$N_{fish-eye} = N_{total} + N_{int} = \frac{\pi E^2}{2(\Delta\sigma)^2} \left[ 1 + (x^3 - 1) \sqrt{\frac{a_0}{a_i}} - x^3 \sqrt{\frac{a_0}{a}} + \frac{1}{2 \left( \frac{\alpha}{2} - 1 \right)} \left[ \left( \frac{a_0}{a_{int}} \right)^{\left( \frac{\alpha}{2} - 1 \right)} - 1 \right] \right]$$

Considering that  $a_{int}$  could be a few percent less than an initial crack  $a_0$  with the logarithmic crack growth slope  $\alpha$  of the order of 100, it is found that  $N_{int}$  is very small compared to  $N_{total}$ . Thus, in first approximation  $N_f = N_{total}$

### Gigacycle Fatigue of a PM Nickel Base Alloy (N18)

In order to study the application of this model to the effect of defects, we have chosen a powder metallurgy nickel base alloy (N18) with and without seeding of inclusions. The chemical composition of N18 nickel base alloy is:



The principal mechanical properties are:

$$\sigma_y = 1050 \text{ MPa}$$

$$UTS = 1500 \text{ MPa}$$

In order to reveal the effect of defects, seeding with ceramic inclusions (80 to 150  $\mu\text{m}$  diameter) was made, using 30 000 inclusions for 1 kilogram of alloy. A comparison is done between N 18 alloy with and without seeded inclusions. Nevertheless, it is observed that when the rate of ceramic particles increases, the porosity is also increased that is to say a competition exists between particles and pores for crack nucleation.

*Fatigue Crack Growth of N18 Alloy*

The figure 4 presents the results at high frequency for  $R=-1$ . One can see that the threshold is smaller to high temperature that at ambient temperature. Normally we could expect a fall of threshold with the increase of the temperature. But on the figure 4 the threshold is smaller at 400°C that at 650°C and 750°C. The curves at 400°C, at 650°C and 750°C cut the vicinities  $10^{-5}\text{mm/cycle}$ . The observed gaps are explained by the phenomenon of oxidization on the surface of crack. On the crack surface of the sample used in our tests, oxidization at 650°C and at 750°C was observed. At high temperature, normally the crack rate propagation increases with the temperature. But the oxidization might slow down propagation in the neighborhood threshold when the temperature is rather elevated. (5)

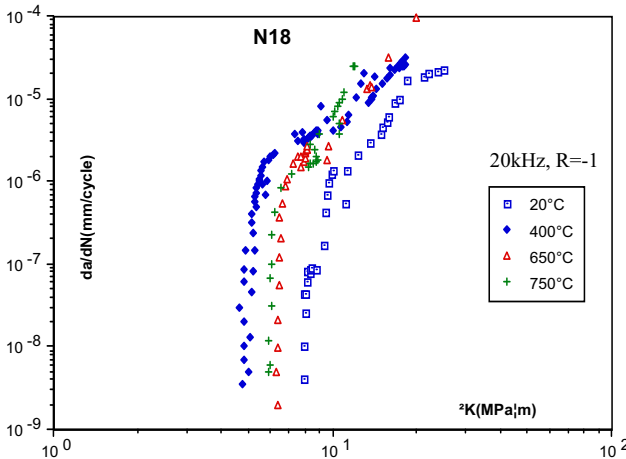


Figure 4 – Fatigue threshold for N18 at  $R = -1$

We found that the  $\Delta K$  thresholds for  $R = -1$ ,  $R = 0$ ,  $R = 0,8$  are respectively 5,5 8 and 4,2.  $\text{MPa}\sqrt{\text{m}}$ , at 450°C which is the normal temperature of a turbine disk.

*Fatigue crack initiation of N18 alloy*

Figure 5 presents the fatigue results on N18 nickel base alloy at 20 kHz with different ratios  $R$ . The specimens were polished before testing. There is no horizontal asymptote on the S-N curve between  $10^6$  and  $10^7$  cycles. Between  $10^6$  and  $10^9$  cycles the S-N curves have a uniform decreasing slope is observed. It means that the fatigue limit defined as an asymptotic value of the stress up to  $10^6$  is a wrong concept in this case. It is found that for long life range the initiation of the crack starts inside the specimen from a defect. It means that the number of cycles so-called for initiation depends of the size of the defect, the location of the defects and also perhaps on low crack growth rates in vacuum, before the internal crack reaches at the surface of the specimen.

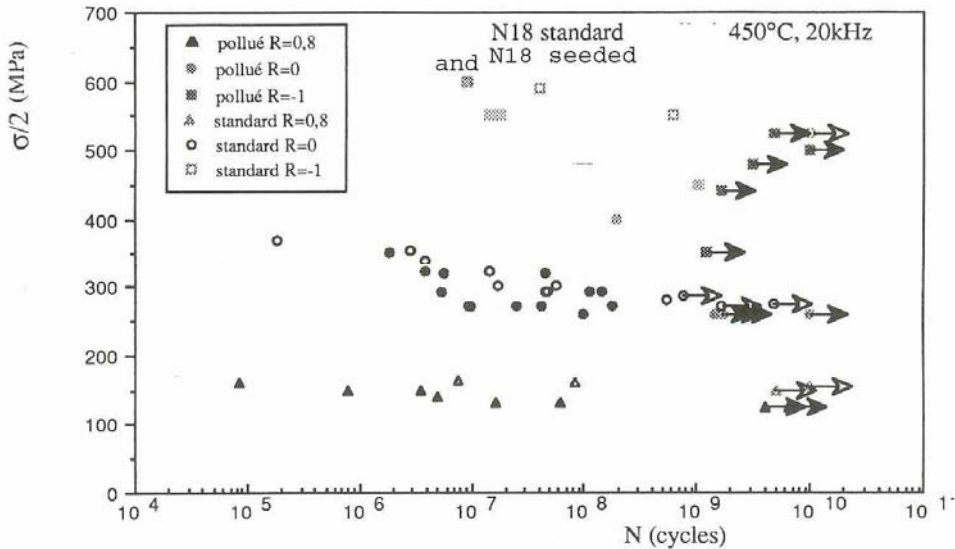


Figure 5 – SN curves for N18, standard and seeded, at 450°C

At  $R=-1$ , the fatigue strength at  $10^9$  cycles of the standard material is 525 MPa. But in presence of inclusions the fatigue limit can drop below 400 MPa.

The curve of standard and seeded N18 with  $R=0$  are shown figure 5. Initiation sites are mainly porosities for the standard N18 and ceramics inclusions for seeded material inside the sample and not on surface. The data scattering for seeded material is higher than standard because of the size, shape and interfaces with the matrix of porosities. But it is outstanding that fatigue limits are not so different (270MPa for standard material and 260MPa for the seeded one) although that the average size of porosities and inclusions are quite different (23 $\mu$ m for standard and 98 $\mu$ m for seeded).

It is also observed that for the standard SN curve, the fatigue limit at  $10^9$  cycles is 75 MPa lower than fatigue limit at  $10^6$  cycles.

At  $R=0.8$ , the fatigue strength of seeded material is 25 MPa lower than standard material (125 MPa for standard and 150 MPa for seeded). A large mean stress value increases the ceramic inclusion effect.

#### Mechanisms of the gigacyclic fatigue of N18 alloy

In the literature, few results are given on this topic. According to our own observations and those of Murakami (7), the gigacyclic fatigue crack initiation occurs essentially inside the sample and not at the surface as it is observed for shorter lives at higher stresses.

At lower stresses, we can expect crack initiation from the existing defects which nucleate a fish eye.

As an example, we consider the specimens failed at 291 MPa and  $R=0$  (figure 5) after  $10^8$  cycles. The average size of the defect in the middle of the fish eye is 100 $\mu$ m, for a fish eye diameter of final size 1200 $\mu$ m. The maximum size of the defect (more or less an ellipse) is 165 $\mu$ m.

According to the relations given previously, it is found that  $N_f$ , the number of cycles of propagation to develop the full fish eye is approximately  $7.3 \cdot 10^5$  cycles. This means that the number of cycles of initiation is much more important than the propagation of the crack.

Now, considering the threshold concept, the initial  $\Delta K_i$  at the tip of the defect is found between 3.28 and 4.21  $\text{MPa}\sqrt{\text{m}}$ , depending on the average or maximum size of the defect. This is less or equal to the fatigue threshold of a short crack in such alloy at 450°C (figure 4). Therefore it means that the crack growth rate is of the order of  $10^{-6}$  mm/cycle or higher, following the results of figure 4. In these conditions the number of cycles of propagation to develop a fish eye of 600µm radius should be around  $6 \cdot 10^5$  cycles in good agreement with  $N_f$  computed above.

## Conclusion

In the gigacycle regime of PM N18 nickel based alloy used for turbine disks, the fatigue strength is related to the initiation of permanent slip bands around defects more than crack growth. Comparing the effect of inclusions and porosities in the N18, it is interesting to point out the following:

The role of the inclusions is sometimes hidden by the role of porosities when the R load ratio is equal to -1 or to 0. The scattering of the results for  $R = 0$  in a N18 seeded with ceramic inclusions is important, since for a N18 standard, the scattering is low.

It is very remarkable that when  $R = 0$ , the resistance to gigacycle fatigue at 450°C is about 250 MPa in the N18 with or without inclusions. The porosity is dominant.

On the contrary, when the mean stress of the fatigue cycle is very high, for  $R = 0.8$ , the role of inclusions becomes preponderant. Without inclusions, the N18 fatigue limit, at 450°C, is 155 MPa at  $10^9$  cycles. However, it is 125 MPa with inclusions.

This is the case of the damage done by the vibrations on the turbine disks for which a better design could be obtained using both LCF and VHCF analysis methods.

*Acknowledgements: The authors are grateful for the financial support of SAFRAN/SNECMA.*

## References

1. P. Lukas and al. Fatigue behaviour of ultrafine-grain copper in VHCF regime. VHCF4 2007, Ann Arbor, 265-270
2. H. Mughrabi and S. Stanzl. Fatigue damage evolution in ductile single phase FCC metals in the UHCF regime. VHCF4, 2007, 75-82
3. C. Bathias and PC Paris. Gigacycle Fatigue in mechanical practice. M. Dekker Publisher 2005
4. C. Bathias There is no Infinite Fatigue Life in Metallic Materials. Fat. Fract. Eng. Mat. Struct (1999), 22, 559-565
5. J. Bonis, Thèse de doctorat, Univ. Paris-Sud, 1997
6. T. Wu and C. Bathias., "Application of fracture mechanics concept in ultrasonic fatigue" Eng.. Fract. Mech., Vol. 47, No 5, pp 683-690, 1994.
7. Y. Murakami and M. Endo., "Effects of defects, inclusions and in homogeneities on fatigue strength", Fatigue, Vol. 16, 163-182, 1994